JOURNAL OF OPTOELECTRONICS AND ADVANCED MATERIALS Vol. 10, No. 4, April 2008, p. 813 - 818

Nanoparticle sizing by coherent light scattering – computer simulation results

D. CHICEA
Physics Department, University Lucian Blaga of Sibiu, Dr. Ion Ratiu Str. 7-9, Sibiu, 550012, Romania

If coherent light is incident on a fluid having nanoparticles in suspension the result of the far field interference is a "speckled" image. In a suspension the SCs have a complex movement of both sedimentation and the Brownian motion. As a result of the SCs permanent position changes the speckle image is not static but presents time fluctuations. A computer code to simulate both the static and the dynamic properties of the coherent light scattering on nanofluids was written, tested and used to calculate the far field intensity variation for nanofluids having different particle size. The results are discussed and an experimental method for fast nanoparticle size assessing is suggested.

(Received February 25, 2008; accepted April 2, 2008)

Keywords: Nanoparticles, Computer simulation, Image processing

1. Introduction

The nanofluid was first mentioned by Choi in 1995 [1] as he noticed that a small amount of nanoparticles, added in a fluid, considerably enhanced the heat transfer properties [2].

The irregular, complex nanoparticle motion in the fluid, which consists of sedimentation and Brownian motion, is the cause of the remarkable enhancement of heat transfer properties of the nanofluids [3-6]. The irregular motion directly depends of the particle dimension therefore particle velocity techniques might furnish information on the nanoparticle size.

Measuring the nanoparticle velocity resembles much measuring the velocity distribution of flow field by seeding fluids with small particles, like the particle image velocimetry, laser Doppler velocimetry and laser speckle velocimetry techniques, therefore the computer experiment presented in this work considers a speckle analysis technique [7], [8].

The seeding particles must scatter enough light to produce a good signal-to-noise ratio in order to be proper for laser particle velocimetry, therefore the diameter of the seeding particle is typically in the micrometer range. The nanoparticles though have a much smaller diameter, around 10 nanometers [9] and the intensity of the scattered light is much smaller. Experimental work was done on coherent light scattering by nanoparticles and results were reported in papers like [10] and [11].

In this work a program to simulate light scattering by nanoparticles is described and the results of the simulation for nanoparticles with different diameters are presented. The computer simulation presented here is essentially different of other computer simulations, because the individual motion of each nanoparticle in suspension is considered and the far interference field is calculated by adding the contribution of the wavelets scattered by each nanoparticle, without using average optical properties of finite volume elements, like most of the simulations [12], [13]. Each nanoparticle in suspension was individually considered and moved, using a Monte Carlo type algorithm. The time step used in simulating the nanoparticle Brownian motion was assessed using a diffusion computer experiment and by comparing the simulation data with the experimental diffusion data, thus the nanoparticle motion is as realistic as possible. Details on assessing the simulation time step, on the algorithm of moving each nanoparticle in suspension and of simulating the dynamics of the light scattering on nanoparticles in suspension are presented in the next section.

2. The algorithm

If coherent light is incident upon a medium having scattering centers (SC hereafter) randomly distributed, an not uniformly illuminated image is obtained, currently named speckled image, as a result of the interference of the wavelets scattered by the scattering centers. The image changes in time as a consequence of the scattering centers complex movement of sedimentation and Brownian motion. This produces fluctuations of the image intensity in each location of the interference field. These fluctuations give the "boiling speckles" aspect [7] [8]. In this work the objective speckle [7], respectively far field speckle [8] is considered.

2.1 Image calculation details

The program considers coherent light having 632 nm wavelength to be incident on a cuvette containing the suspension. The beam transversal area and light pass are adjusted as input parameters. The far field interference pattern was calculated at a distance D apart from the simulated cuvette, which is considered to be located within the coherence region of the light source. Fig. 1 presents the schematic of the computer simulation setup.

In order to calculate the static far field intensity distribution (one image) the scattering centers positions were generated in the active volume of the cuvette (beam volume) using random numbers with uniform distribution.

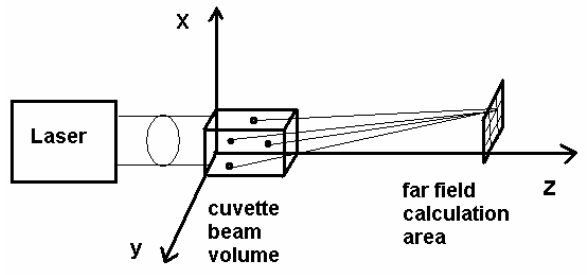

Fig. 1. The schematic of the computer simulation.

The single act light scattering on a SC was modeled using (1) [14], [15]:

$$I(\theta) = I_0 \frac{1+\cos^2\theta}{2R^2}\left(\frac{2\pi}{\lambda}\right)^4\left(\frac{n^2-1}{n^2+2}\right)^2\left(\frac{d}{2}\right)^6 \quad (1)$$

where R is the distance from the nanoparticle to the far field location, θ is the scattering angle, n is the refractive index of the particle, and d is the diameter of the nanoparticle.

The magnitude of the electric field E_0 was considered to be proportional to the square root of I in (1). The complex amplitudes of the electric field intensity scattered by each SC, described by eq. (2), were added on each pixel the calculated image consists of.

$$E(D) = E_0 \exp(i\frac{2\pi}{\lambda}R) \quad (2)$$

A file is written for each calculated image and another program reads all the files, performs an intensity normalization and finally writes another file with the calculated far field for each image, in the desired, conventional graphical format.

2.2 Nanoparticle motion simulation details

For each time step the SCs were moved in the active area considering both the uniform sedimentation and the Brownian motion. The sedimentation motion of the SC carries on with a constant velocity, which is the consequence of the null resultant of three forces: gravity, Archimede's force and the viscous force in laminar flow regime (Stokes). Considering the SC with a spherical shape, the velocity is given by equation (3):

$$v_s = \frac{2r^2 g}{9\eta}\cdot(\rho-\rho_0) \quad (3)$$

where r is the radius of the sphere, ρ is the density of the scattering center, ρ_0 is the density of the fluid, η is the dynamic viscosity coefficient of the fluid. The fluid was considered to be water and the variation of the water density and dynamic viscosity with temperature was calculated by a polynomial fit on the experimental data in [16]. The sedimentation motion was modeled for each SC individually by changing the position with a distance equal with the v_s times the time step on the vertical direction.

The Brownian motion was modeled differently, for each SC type. The Maxwell – Boltzman velocity distribution is actually the product of the three velocity distribution function for one dimension (4):

$$f_v(v_i) = \sqrt{\frac{m}{2\pi kT}}\cdot\exp\left(-\frac{mv^2{}_i}{2kT}\right) \quad (4)$$

In (4) k is Boltzman's constant, T is the absolute temperature, m is the mass of the particle in thermal equilibrium with the environment and i can be either x, y or z. At each simulation time step the velocity values for v_x, v_y and v_z of each SC were therefore generated using random numbers with a normal distribution having the variance kT/m.

It should be noted that in order to have a realistic Brownian motion modeling, the time step for the Brownian motion must be different of the time step used to model the sedimentation and details on assessing it are presented below.

If particles are diffusing in a solvent, the number density $n(\vec{r},t)$ variation in time is described by the basic equation:

$$\frac{\partial n}{\partial t} - D\cdot\nabla^2 n = 0 \quad (5)$$

also called the diffusion equation, where D is the diffusion coefficient. Since the probability $P(\vec{r},t)$ of finding a particle in a small volume is directly proportional to the number density, this leads to the equation (6)

$$\frac{\partial P}{\partial t} - D\cdot\nabla^2 P = 0 \quad (6)$$

The diffusion coefficient D can be related to other properties of the system like the temperature T and μ, the mobility, which is the ratio of drift velocity to driving force when the particle is pushed through the fluid by an external force, by invoking the Einstein relation:

$$D = k_B T\mu \quad (7)$$

The mobility can be calculated from classical hydrodynamics for spheres of radius R which are large compared to the surrounding molecules, driven by an external force $F_{ext,}$ in laminar flow regime (Stokes):

$$\vec{F}_{ext} = 6\pi\eta R\vec{v}_{drift}, \quad \vec{v}_{drift} = \mu\cdot\vec{F} \quad \Rightarrow$$
$$\mu = \frac{1}{6\pi\eta R} \quad (8)$$

Substituting μ in (7) we find the diffusion coefficient for spheres of radius R_0 to be:

$$D = \frac{k_B T}{6\pi\eta R_0} \tag{9}$$

We want a solution to this equation with the initial condition that the particle is at $r = 0$ at $t = 0$:

$$P(0,0) = \delta(\vec{r}) \tag{10}$$

Such a solution, that can be can be proved by direct differentiation is:

$$P(\vec{r},t) = (4\pi D t)^{-\frac{3}{2}} \cdot \exp\left(-\frac{r^2}{4Dt}\right) \tag{11}$$

The result from the diffusion equation, the probability distribution $P(\vec{r},t)$ must be connected with a real measurable quantity. The second moment of the P distribution, $\langle r^2 \rangle$ draws a useful relationship about diffusion and taking advantage of the radial symmetry and using polar coordinates we find:

$$\langle r^2(t) \rangle = \int_0^\infty \int_0^\pi \int_0^{2\pi} r^2 \cdot P(\vec{r},t) \cdot r^2 \cdot \sin\theta d\theta d\varphi = 6Dt \tag{12}$$

First a set of simple computer diffusion experiments was done. 5000 nanoparticles were used in order to have a good statistics and their positions were (0,0,0) in cartezian coordinates at time t=0. A certain value was selected for the Brownian motion time step modeling and the system was let to evolve for a total preselected time t. At each time step the particles velocities were generated having a Maxwell – Boltzman velocity distribution, described by (4) and the new positions were calculated for each particle adding to the old positions the velocity times the time step. When the preset time elapsed, the positions were saved, $<r^2>$ was computed and finally D_{comp} was calculated from (12) for that particular value of the time step. Different time step values were used for each experiment, a curve was drawn with D_{comp} values versus the time step. The time step value that produced a Dcomp value equal to the one calculated with (9) was chosen for the light scattering dynamics simulation.

For 10 nm nanoparticles in water at 293.15 K the diffusion coefficient calculated with (9) is 4.2781×10^{-11} m^2s^{-1} and the Brownian motion time step produces a D_{comp} that matches this value is 6.0803×10^{-11} s. Other details on the receipt for determining the Brownian motion time step are presented in [17].

The sedimentation motion velocity is roughly 10^9 times smaller than the Brownian motion [17]. This proves that the Brownian motion is the main cause of the speckle fluctuations for a nanofluid as target.

There does exist another major cause of the light intensity fluctuations in each location of the interference field, beyond the constant phase change of the wavelets emitted by each SC, namely the variation of the number of SCs in the beam area. In order to do a realistic simulation this fluctuation cause was coded as well, by increasing the initial volume the nanoparticles were generated into, accordingly to the sedimentation motion and to the diffusion during the time span of the experiment, keeping the average nanoparticle concentration constant; further details are presented in [17].

The program can be used to compute either an image of the far field, or a movie, with the desired framerate and resolution, in a certain location of the far field, or the time series of the light intensity recorded by a detector with a certain dimension and location in the far field. Results of the computer simulations are presented in the next section.

3. Simulation results

First the control parameters were adjusted to calculate a far field image. A far field computed image having 10 nm diameter nanoparticles as target is presented in Fig. 2.

The image has a speckled aspect, exactly as a far field intensity recorded during a laboratory light scattering experiment on diluted nanofluid.

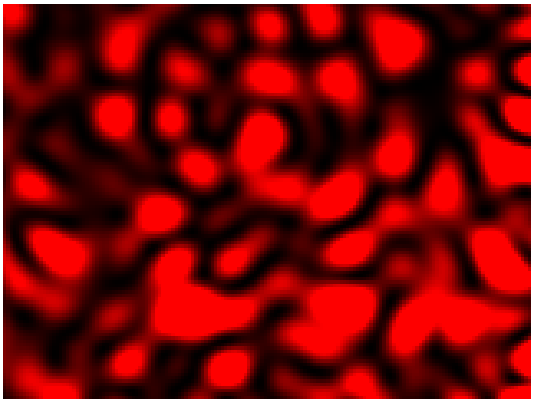

Fig. 2. A computed far field image movie having 10 nm diameter nanoparticles as target.

Fig. 3 presents the 3D distribution of the intensity of the bitmap presented in Fig. 2 over the 160×120 pixels the image consists of. The image in Fig. 2 and the intensity distribution in Fig. 3 are in good agreement with the computer simulation in [11].

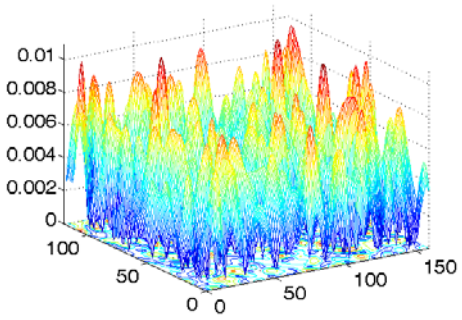

Fig. 3. a 3D intensity distribution of the bitmap in Fig. 2.

First the computer experiment was conducted in such a manner to investigate the static parameters (average intensity, average contrast and average speckle size) variation with the particle diameter. The cuvette-detector distance was 0.8 m, the detection area was 0.005 m apart from the beam direction, at an angle of 0^o 21' 30''.

During a nanofluid synthesis the average particle dimension is not known precisely, as it strongly depends of the fabrication process parameters [3], [19]. The nanofluid can be diluted and the volume ratio after dilution can be defined as:

$$f_v = \frac{V_{nano}}{V} \tag{13}$$

In (13) V_{nano} is the total volume of the nanoparticles and V is the total volume of the suspension.

The volume ratio can be experimentally adjusted precisely for a sample, therefore the computer experiment considered different samples having the same volume ratio but different particle diameters, hence different SC physical parameters and number. For each type of suspension a bitmap image was calculated, having a volume ration of $5.0*10^{-13}$ and particle diameters from 10 to 60 nm. Additional details on the program that was written and used to calculate the static far field parameters and the procedure used to calculate them are presented in [18] and [19]. The average intensity variation with the particle diameter, for samples having a constant volume ratio, is presented in Fig. 4.

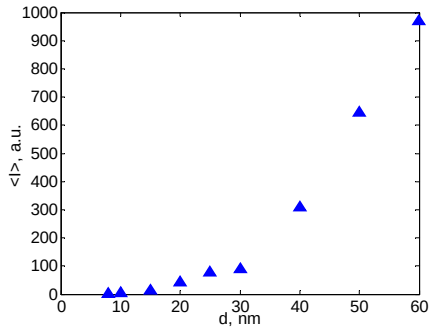

*Fig. 4. The average intensity variation with the particle diameter, for samples having a volume ratio equal to 5.0*10-[13].*

Examining Fig. 4 we notice a constant increase of the average intensity with increasing the particle size, especially in the small nanoparticle size range, which is of interest for biomedical applications [20].

The increase of the average intensity $<I>$ value with the nanoparticle size is in good agreement with the theory. As the particle diameter d increases, at constant volume ratio the nanoparticles N number should vary with the diameter d as:

$$N = \frac{V_{nano}}{\frac{4\pi}{3}\cdot\left(\frac{d}{2}\right)^3} \tag{14}$$

Light scattering on nanoparticles is a Rayleigh type scattering, therefore the light intensity scattered by one individual particle is proportional to d^6 [14] (1). The average intensity scattered by all the nanoparticles in the sample and recorded at a constant angle is therefore proportional to d^3, thus increasing with the nanoparticles diameter, as revealed by eq, (15).

$$< I >= N < I(\theta) > \approx \left(\frac{d}{2}\right)^3 \tag{15}$$

This variation of the average intensity with the nanoparticle diameter, at constant volume ratio suggests a fast and low cost procedure to assess the nanopatticle diameter, as described in the next section.

The average contrast and the average speckle size variation with the particle size is not as strong as the average intensity variation, therefore they are not presented here.

The second type of computer experiment consisted of running the program with another value of the control parameter, in order to calculate a time series representing the far field intensity fluctuation. The cuvette-detector configuration was the same as in the previous experiment. A 0.2 second sequence of a time series calculated for a target consisting of 10 nm diameter nanoparticles is presented in Fig. 5.

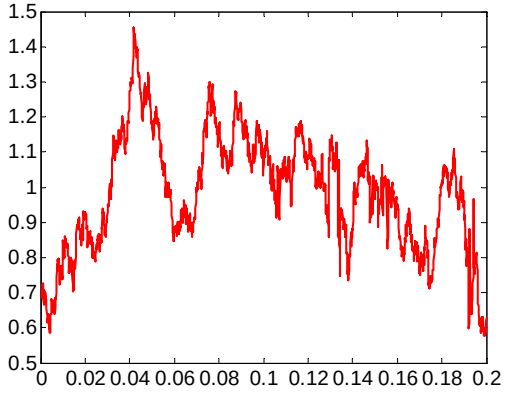

Fig. 5. A calculated time series for of 10 nm diameter nanoparticles.

The autocorrelation function of each of the generated time series was calculated with (16) [21]:

$$A(\tau)=\frac{\langle I(\vec{r},t)\cdot I(\vec{r},t+\tau)\rangle}{\langle I(\vec{r},t)\cdot I(\vec{r},t)\rangle} \tag{16}$$

where the angle brackets denote averages over time *t, r* represents the position of the detector, and τ is the correlation time. The normalized autocorrelation function decreases from 1 and we can define the autocorrelation time τ_c as the time when the autocorrelation function decreases to 1/e.

When the fluid is flowing the SCs have a velocity *v*. The autocorrelation time has a variation with the particle in suspension velocity given by equation (17) [7], [8]:

$$\tau_c=\frac{A}{k\cdot v} \tag{17}$$

where *k* is the wave number and *A* is a constant depending on the scattering properties of the sample. The program was run for particles with a diameter in the range 4 – 37 nm and produced time series for each target. The autocorrelation time was calculated for each target. The sampling rate of the assumed data acquisition system was 10000 per second. The computer time required to produce a time series is very big, as the motion of each SC is individually calculated and tracked, growing linearly both with the length of the time series and with the SC number.

The variation of the autocorrelation time with the SC diameter is presented in Fig. 6. Examining Fig. 6 we notice that the calculated data has a relatively big spread. Nevertheless, an increase of the autocorrelation time with the size of the nanoparticles is obvious.

With the increase of the diameter the particle mass m increases and the velocity in (6) decreases. Consequently τ_c in (19), which was derived considering particles with velocities in one direction, decreases.

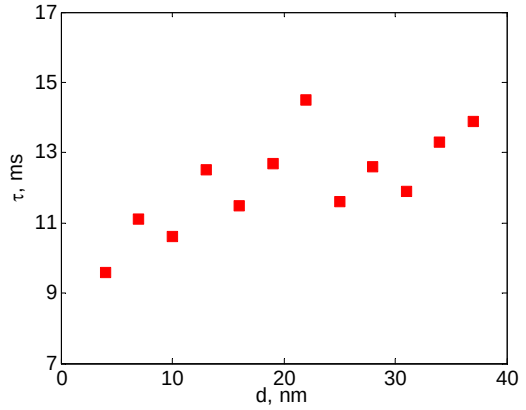

Fig. 6. The autocorrelation time variation with the SC diameter.

We found from this computer experiment that the autocorrelation time τ_c has same trend of decreasing with the increasing of the nanoparticle diameter although the velocity vector for nanoparticles is randomly oriented, rather than in one direction, as was considered when deriving (7). This result is in very good agreement with the literature [15], [22] and is already implemented in commercially available equipment used for nanoparticle sizing [23], [24]. We view this result as another confirmation that the computer simulation described in this paper produces realistic results.

4. Conclusion

The results of the computer simulation presented above were compared with the images and time series recorded during a light scattering experiment on nanofluids. The time series computed during the computer experiment were analyzed and the autocorrelation function was calculated and compared with the autocorrelation function of a time series recorded during a laboratory experiment performed on the real system with the same parameters, as reported in the literature [15], [23], [24].

Running the computer simulation we found that the autocorrelation time of a calculated time series decreases with the increase of the nanoparticle size. This result is a confirmation that the computer simulation, which describes accurately both the far field interference aspect and the light scattering dynamics, produces realistic results.

The nanoparticle size is one of the most important parameters that dictate the properties of a nanofluid or magnetic fluid. The computer simulation results presented in this work suggest a simple and low cost procedure for assessing the nanoparticle size. It requires a measurement and time averaging of the scattered light intensity at constant angle and, most important, at constant volume ratio, which can be adjusted accurately with common laboratory equipment. A calibration curve is drawn first using nanoparticles with a precisely known diameter, measured using TEM or other conventional method. The curve can be used later on in measuring the nanoparticle diameter for a new prepared sample, after diluting a small amount of it to the same volume ratio used in calibration.

It should be noted though that the method for nanoparticle diameter assessment suggested in this section is not related with the Dynamic Light Scattering (DLS) techniques because it does not use the light scattering dynamics. Light scattering dynamics was used to validate the results and to verify that they are realistic. The plot in Fig. 4 presents time averages of the light scattered at a certain angle, thus involving static not dynamic light scattering. For this reason the average intensity is connected with the physical diameter of the nanoparticle not with the hydrodynamic diameter, as in DLS techniques.

Experimental work is scheduled to verify the proposed method.

References

[1] U. S. Choi, ASME Fed. **231**, 99-103 (1995).
[2] P. Vadasz, J. Heat Transfer. **128**, 465-477 (2006).
[3] S. P. Jang, S. U. S. Choi, Appl. Phys. Lett. **84**, 4316-4318 (2004).
[4] W. Evans, J. Fish, P. Keblinski, Appl. Phys. Lett. **88**, 093116 (2006).
[5] Y. M. Xuan, W. Roetzel, Int. J. Heat Mass Transfer. **43**, 3701-3707 (2000).
[6] R. Prasher, P. Brattacharya, P. E. Phelan, Phys. Rev. Lett. **94**, 025901 (2005).
[7] J. W. Goodman, in Laser speckle and related phenomena, Vol. 9 in series Topics in Applied Physics, J. C. Dainty, Ed., Springer-Verlag, Berlin, Heidelberg, New York, Tokyo, (1984).
[8] J David Briers, Physiol. Meas. **22**, R35–R66 (2001).
[9] W.-X. Fang, Z.-H. He(a), X.-Q. Xu, Z.-Q. Mao, H. Shen, European Physics Letters **77** 68004-68009, (2007).
[10] Dan Chicea, Mihaela Răcuciu, accepted to be published in J. Optoelectron. Adv. Mater. **9**(8), (2007).
[11] Ming Qian, Jun Liu, Ming-Sheng Yan, Zhong-Hua Shen, Jian Lu, Xiao-Wu Ni, Optics Express **14**(17), 7559 (2006).
[12] L. Wang, S. L. Jacques, L. Zheng, MCML – Monte Carlo Modeling of light transport in multi-layered tissues, Computer Methods and Programs in Biomedicine **47**, 131 (1995).
[13] S. A. Prahl, M. Keijer, S. L. Jacques, A. J. Welch, A Monte Carlo Model of Light Propagation in Tissue, SPIE Proceedings Series, IS **5**, 102 (1989).
[14] C. F. Bohren, D. Huffman, Absorption and scattering of light by small particles, John Wiley, New York (1983).
[15] W. Tscharnuter, Photon Correlation Spectroscopy in Particle Sizing, in Encyclopedia of Analytical Chemistry, R. A. Meyers (ed), 5469, John Wiley & Sons Ltd, Chichester (2000).
[16] http://www.thermexcel.com/english/index.htm
[17] D. Chicea, Proc. IBWAP-7, submitted to JOAM.
[18] D. Chicea, Romanian Journal of Physics, **52**(5-6), 589 (2007).
[19] D. Chicea, European Physical Journal Applied Physics **40**, 305 (2007).
[20] Q. A. Pankhurst, J. Connolly, S. K. Jones, J. Dobson, J. Phys. D, **36,** R167 (2003).
[21] R. Bracewell, The Fourier Transform and Its Applications, 3rd ed. New York: McGraw-Hill, pp. 40-45 (1999).
[22] N. Zhelev, S. Barudov, Biotechnol. & Biotechnol. Eq. **19**, 3 (2005).
[23] http://www.malvern.co.uk
[24] http://www.bic.com/

*Corresponding author: dan.chicea@ulbsibiu.ro